Available online at www.sciencedirect.com
SCIENCE DIRECT®
Journal of Solid State Chemistry 177 (2004) 916–921
JOURNAL OF SOLID STATE CHEMISTRY
http://elsevier.com/locate/jssc

$K_2Mo_4O_{13}$ phases prepared by hydrothermal synthesis

Kazuo Eda,[a,*] Kin Chin,[a] Noriyuki Sotani,[a] and M. Stanley Whittingham[b]

[a] *Department of Chemistry, Faculty of Science, Kobe University, Nada-ku, Rokko-dai, Kobe 657-8501, Japan*
[b] *Institute for Materials Research, State University of New York at Binghamton, Binghamton, NY 13902-6000, USA*

Received 22 July 2003; received in revised form 21 September 2003; accepted 24 September 2003

Abstract

Hydrothermal synthesis in the K–Mo oxide system was investigated as a function of the pH of the reaction medium. Four compounds were formed, including two $K_2Mo_4O_{13}$ phases. One is a new low-temperature polymorph, which crystallizes in the orthorhombic, space group *Pbca*, with $Z = 8$ and unit cell dimensions $a = 7.544(1)$ Å, $b = 15.394(2)$ Å, $c = 18.568(3)$ Å. The other is the known triclinic $K_2Mo_4O_{13}$, whose structure was re-determined from single crystal data; its cell parameters were determined as $a = 7.976(2)$ Å, $b = 8.345(2)$ Å, $c = 10.017(2)$ Å, $\alpha = 107.104(3)^\circ$, $\beta = 102.885(3)^\circ$, $\gamma = 109.760(3)^\circ$, which are the standard settings of the crystal lattice. The orthorhombic phase converts endothermically into triclinic phase at ca. 730 K with a heat of transition of 8.31 kJ/mol.

Keywords: Hydrothermal synthesis; Molybdate; Crystal structure; $K_2Mo_4O_{13}$

1. Introduction

As is now well-known, hydrothermal syntheses can lead to the formation of materials at much lower temperatures than those necessary in solid-state syntheses. Some of these low-temperature reactions may go through intermediate states, which keep a structural resemblance to the starting compound. Thus, in such cases it may be possible to control the key elements of the structure of the product by varying the structure of the starting material; it is likely that at least part of the starting material remains in the solid state throughout the hydrothermal synthesis, acting as something like a template or a nucleus for the new compound. We successfully used this approach in the hydrothermal preparation of the alkali metal molybdenum bronzes. Thus, when $H_{0.28}MoO_3$ was the suspended solid the blue molybdenum bronze $K_{0.30}MoO_3$ was formed, while starting with $MoO_{2.86}$ or with a mixture of $0.86MoO_3 + 0.14MoO_2$ gave the red molybdenum bronze $K_{0.33}MoO_3$ (together with a small amount of by-product) [1,2]. The $MoO_{2.86}$ was prepared by heat-treating $H_{0.28}MoO_3$ in N_2.

In this study, we attempted to apply similar solid-containing hydrothermal syntheses to the preparation of fully oxidized molybdates (Mo^{VI}). However, the products formed did not depend on whether the starting system contained any solid phase, probably because Mo^{VI} species have higher solubility, resulting in complete dissolution of the starting solids under hydrothermal conditions. We did find and characterize a new $K_2Mo_4O_{13}$ phase and present the details here, and re-evaluated triclinic $K_2Mo_4O_{13}$ (hereafter named t-$K_2Mo_4O_{13}$). We did not find the reported monoclinic $K_2Mo_4O_{13}$ (m-$K_2Mo_4O_{13}$).

2. Experimental

About 0.287 g of MoO_3 (2 mmol) was suspended in 30 mL of an aqueous 2.40 M KCl solution. The pH value of the solution was controlled by adding HCl or KOH solution: HCl was added for solution with pH values <2.1, while KOH was added for solution with pH values >2.1. The solution was put into a 60 mL Teflon-lined autoclave and heated in a forced convection oven at 433 K under autogenous pressure for 1 day. The resulting product was filtered, washed with distilled water, and dried in air at room temperature.

*Corresponding author. Fax: +81-78-803-5677.
E-mail address: eda@kobe-u.ac.jp (K. Eda).

0022-4596/$ - see front matter © 2003 Elsevier Inc. All rights reserved.
doi:10.1016/j.jssc.2003.09.029

X-ray powder and single crystal diffraction data of the products formed were collected on a Mac Science MXP3VZ X-ray diffractometer with a graphite monochromator using Cu$K\alpha$ radiation or on a Bruker smart1000 diffractometer with a CCD detector using graphite monochromated Mo$K\alpha$ radiation. The structure of the single crystal was solved by direct method and refined by full-matrix least-squares calculations based on F_o and F_o^2 with empirical absorption corrections using Bruker SHELXTL programs. The density of the product was measured by picnometry. The composition of the product was determined by a HITACHI 180-80 atomic absorption spectrometer using the 313.3 nm line for Mo and 766.5 nm for K. Thermogravimetric and differential thermal analyses (TG–DTA) were performed in air on a Mac Science TG–DTA 2010S system at a heating rate of 10 K/min. The heat absorbed at the phase transition was measured using a Mac Science DSC 3100SA system at a heating rate of 5 K/min.

3. Results and discussion

3.1. Products of hydrothermal syntheses

The materials formed depend on the pH of the starting solution, and their X-ray powder patterns are shown in Fig. 1. Four phases were identified. Three of these were identified through the ICDD files as known phases: MoO_3 [3], potassium decamolybdate $K_2Mo_{10}O_{31}\cdot 5H_2O$ [4], and t-$K_2Mo_4O_{13}$ [5]. These were formed as a main product in the ranges of $pH \leqslant 1.1$, $1.3 \leqslant pH \leqslant 1.6$, and $4.5 \leqslant pH \leqslant 5.2$, respectively. No solid product was obtained at pH values exceeding 5.3. The fourth phase was obtained as a main product in the range $1.7 \leqslant pH \leqslant 4.4$ and was prepared as a single phase in ca. 60% yield at $pH = 2.1$. Its X-ray pattern did not match any pattern reported by ICDD. The pattern could be fully indexed with an orthorhombic cell ($a = 7.562(3)$ Å, $b = 15.421(7)$ Å, $c = 18.620(13)$ Å).

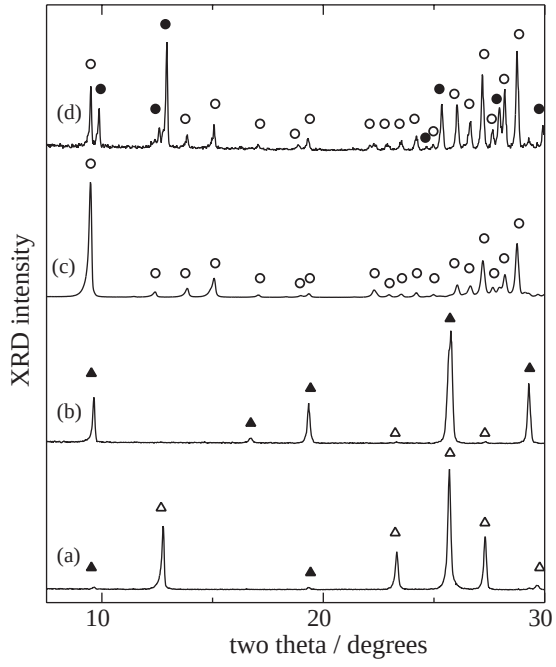

Fig. 1. XRD patterns of hydrothermal products prepared under various pH conditions: pH = 1.1 (a), pH = 1.4 (b), pH = 2.1 (c), and pH = 4.7. Symbols △, ▲, ○, and ● indicate MoO_3, potassium decamolybdate, the new orthorhombic phase, and t-$K_2Mo_4O_{13}$, respectively.

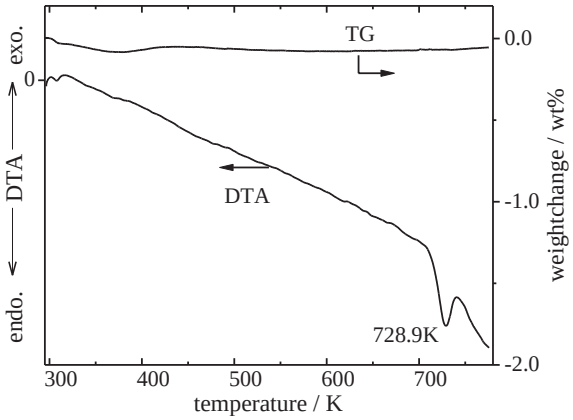

Fig. 2. TG–DTA curves of the new orthorhombic phase.

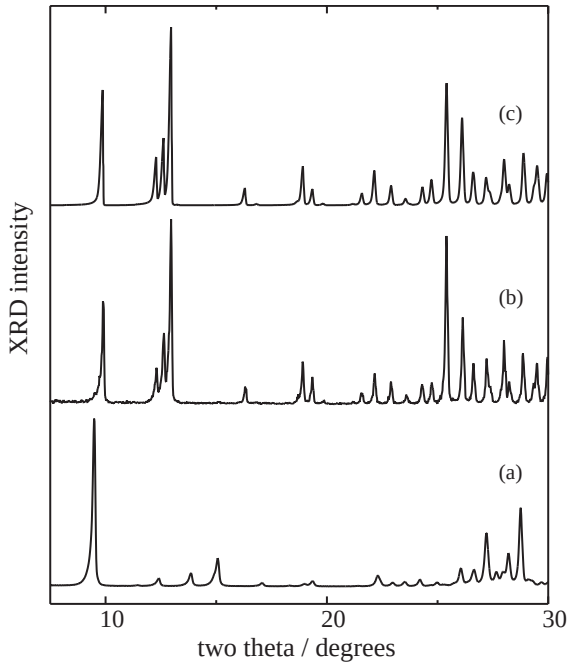

Fig. 3. X-ray powder diffraction pattern of the new orthorhombic phase (a) before and (b) after heating in air at 773 K. The pattern (c) calculated from the structural data of Gatehouse et al. [5] for t-$K_2Mo_4O_{13}$ is shown for comparison.

Table 1
Crystallographic data for t-$K_2Mo_4O_{13}$

Atomic coordinates and thermal parameters						
Atom	Site	Occupancy	x	y	z	U_{eq}
Mo(1)	2*i*	1.0	0.81011(8)	0.50375(7)	1.04828(6)	0.00920(15)
Mo(2)	2*i*	1.0	0.82940(8)	0.90744(7)	1.06205(6)	0.01029(15)
Mo(3)	2*i*	1.0	0.77518(8)	0.60279(7)	0.72847(6)	0.01028(15)
Mo(4)	2*i*	1.0	0.77648(8)	0.20295(7)	0.70807(6)	0.01004(15)
K(1)	2*i*	1.0	0.7456(2)	0.7847(2)	0.43592(17)	0.0222(4)
K(2)	2*i*	1.0	0.6894(2)	0.2392(2)	0.3093(2)	0.0287(4)
O(1)	2*i*	1.0	0.6536(7)	0.9386(6)	0.9601(5)	0.0226(11)
O(2)	2*i*	1.0	0.9488(6)	0.8628(6)	0.8825(5)	0.0134(10)
O(3)	2*i*	1.0	0.8991(7)	0.6158(6)	0.6108(5)	0.0194(10)
O(4)	2*i*	1.0	0.7046(6)	0.6306(6)	0.9417(5)	0.0130(9)
O(5)	2*i*	1.0	0.7179(6)	0.5125(6)	1.1856(5)	0.0168(10)
O(6)	2*i*	1.0	0.8730(7)	0.1895(6)	0.5706(5)	0.0202(11)
O(7)	2*i*	1.0	0.6358(6)	0.3415(6)	0.6618(5)	0.0148(10)
O(8)	2*i*	1.0	1.0220(6)	0.7859(6)	1.1425(5)	0.0119(9)
O(9)	2*i*	1.0	0.6780(6)	0.2782(6)	0.9123(5)	0.0138(10)
O(10)	2*i*	1.0	0.6003(6)	−0.0156(6)	0.6465(5)	0.0180(10)
O(11)	2*i*	1.0	0.5883(7)	0.6417(6)	0.6541(5)	0.0199(11)
O(12)	2*i*	1.0	0.9584(6)	0.5114(6)	0.8638(5)	0.0116(9)
O(13)	2*i*	1.0	0.7968(7)	0.9424(6)	1.2288(5)	0.0221(11)

Space group, $P\bar{1}$; Lattice constants, $a = 7.976(2)$ Å, $b = 8.345(2)$ Å, $c = 10.017(2)$ Å, $\alpha = 107.104(3)^\circ$, $\beta = 102.885(3)^\circ$, $\gamma = 109.760(3)^\circ$; V (Å^3), 559.9(2); Z, 2; D_o (g cm^{-3}), 3.98(5); D_c (g cm^{-3}), 3.974.
Measurement temp. = 293(2) K, total reflection number = 2177, reflection number $>2\sigma(I) = 1708$, index range $-4 \leqslant h \leqslant 10$, $-10 \leqslant k \leqslant 10$, $-12 \leqslant l \leqslant 12$, $R_{int} = 0.026$, parameter number = 172, restraint number = 0, R_1(all) = 0.044, $R_1(>2\sigma(I)) = 0.033$, wR_2(all) = 0.083, w$R_2(>2\sigma(I)) = 0.076$, $w = 1/[\sigma(F_o^2) + (0.0408P)^2 + 0.0000P]$, $P = (F_o^2 + 2F_c^2)/3$, Goodness of fit = 0.989.

Table 2
Crystallographic data for o-$K_2Mo_4O_{13}$

Atomic coordinates and thermal parameters						
Atom	Site	Occupancy	x	y	z	U_{eq}
Mo(1)	8*c*	1.0	0.70431(7)	0.36155(3)	0.09817(3)	0.0141(2)
Mo(2)	8*c*	1.0	0.60631(6)	0.56785(3)	0.10716(3)	0.0130(1)
Mo(3)	8*c*	1.0	0.92176(6)	0.22262(3)	0.25053(2)	0.0119(2)
Mo(4)	8*c*	1.0	0.82765(6)	0.43126(3)	0.25638(2)	0.0112(1)
K(1)	8*c*	1.0	0.8920(2)	0.47102(9)	0.91560(7)	0.0249(3)
K(2)	8*c*	1.0	0.2299(2)	0.28459(8)	0.06769(8)	0.0304(4)
O(1)	8*c*	1.0	0.8084(5)	0.3215(2)	0.1851(2)	0.0148(8)
O(2)	8*c*	1.0	0.8861(6)	0.3772(3)	0.0430(2)	0.0216(9)
O(3)	8*c*	1.0	0.9221(5)	0.5156(2)	0.3041(2)	0.0158(8)
O(4)	8*c*	1.0	0.6722(5)	0.6465(2)	0.1808(2)	0.0183(9)
O(5)	8*c*	1.0	0.4224(6)	0.6207(3)	0. 759(2)	0.0209(9)
O(6)	8*c*	1.0	0.7653(6)	0.5866(3)	0.0430(2)	0.0214(9)
O(7)	8*c*	1.0	0.6010(6)	0.2722(3)	0.0636(2)	0.0215(10)
O(8)	8*c*	1.0	0.9294(5)	0.3348(2)	0.3066(2)	0.0148(8)
O(9)	8*c*	1.0	0.5424(6)	0.4492(2)	0.0749(2)	0.0163(8)
O(10)	8*c*	1.0	0.6180(5)	0.4270(2)	0.2936(2)	0.0157(8)
O(11)	8*c*	1.0	1.1353(5)	0.2300(2)	0.2153(2)	0.0154(8)
O(12)	8*c*	1.0	0.7781(5)	0.4797(2)	0.1665(2)	0.0153(8)
O(13)	8*c*	1.0	0.9450(6)	0.1580(3)	0.3238(2)	0.0213(9)

Space group, P_{bca}; Lattice constants, $a = 7.544(1)$ Å, $b = 15.394(2)$ Å, $c = 18.568(3)$ Å, $\alpha = 90^\circ$, $\beta = 90^\circ$, $\gamma = 90^\circ$; V (Å^3), 2156.3(5); Z, 8; D_o (g cm^{-3}), 4.10(5); D_c (g cm^{-3}), 4.128.
Measurement temp. = 293(2) K, total reflection number = 2276, reflection number $>2\sigma(I) = 1851$, index range $-7 \leqslant h \leqslant 9$, $-19 \leqslant k \leqslant 18$, $-20 \leqslant l \leqslant 23$, $R_{int} = 0.041$, parameter number = 172, restraint number = 0, R_1(all) = 0.043, $R_1(>2\sigma(I)) = 0.032$, wR_2(all) = 0.089, w$R_2(>2\sigma(I)) = 0.080$, $w = 1/[\sigma^2(F_o^2) + (0.0565P)^2 + 1.4160P]$, $P = (F_o^2 + 2F_c^2)/3$, Goodness of fit = 1.04.
Further details of the crystal structure investigation can be obtained from the Fachinformationszentrum Karlsruhe, 76344 Eggenstein-Leopoldshafen, Germany, (fax: (49) 7247-808-666; mailto: crysdata@fiz.karlsruhe.de) on quoting the depository number CSD 391225.

Our results essentially agree with the results reported by Komaba et al. [6], whose syntheses were from completely dissolved aqueous K_2MoO_4 solutions, except for the new orthorhombic phase reported here. To ensure that solids in the reaction medium here did not lead to the new phase, we also used a synthesis procedure where all the reactants were initially dissolved and the compositions of reactants were maintained the same. Here a K_2MoO_4+2HCl solution was used instead of solid MoO_3; 2 mmol K_2MoO_4+4 mmol HCl in 30 mL of aqueous 2.27 M KCl solution was used instead of 2 mmol MoO_3 in 30 mL of aqueous 2.40 M KCl solution for the pH 2.1 synthesis. This synthesis also gave the orthorhombic phase and so solids in the reaction medium are not necessary for the formation of the orthorhombic phase.

3.2. Relation of the orthorhombic phase to t-$K_2Mo_4O_{13}$

In order to better understand the new orthorhombic phase, its thermal behavior was investigated. The TG–DTA curves in air are shown in Fig. 2. This phase shows essentially no weight change over the entire temperature range studied, but an endothermic peak is observed at ca. 730 K. This phase change was not reversed on cooling. A further endothermic peak is observed at 840 K, where the sample melts. The identity of the phase formed at 730 K was determined through X-ray diffraction of a sample heated to 773 K. This powder pattern is compared with that of the starting material in Fig. 3. All lines can be indexed as t-$K_2Mo_4O_{13}$, which is consistent with no weight change being observed. This suggests that the orthorhombic phase is a polymorph of t-$K_2Mo_4O_{13}$. Atomic absorption analysis showed that the two phases have essentially the same chemical composition: the K and Mo contents were 11.0 and 55.4, 11.4 and 55.9 wt%, 11.7 and 57.3 wt%, respectively for the orthorhombic phase, triclinic phase and calculated for $K_2Mo_4O_{13}$.

We conclude that the orthorhombic phase is a new polymorph of $K_2Mo_4O_{13}$, as its XRD pattern is quite different from t-$K_2Mo_4O_{13}$ [5] and m-$K_2Mo_4O_{13}$ [7,8] phases reported to date. Under the synthesis conditions used here, we did not find m-$K_2Mo_4O_{13}$. The orthorhombic $K_2Mo_4O_{13}$ (hereafter named o-$K_2Mo_4O_{13}$) is not a thermodynamically metastable phase, because it endothermically converts to t-$K_2Mo_4O_{13}$ on heating. Holding t-$K_2Mo_4O_{13}$ at 673 K, 57 K below the transition temperature, for a day did not result in the formation of o-$K_2Mo_4O_{13}$. The transition back from t-$K_2Mo_4O_{13}$ to o-$K_2Mo_4O_{13}$ seems to be kinetically very sluggish. Using DSC analysis, the heat of transition from o-$K_2Mo_4O_{13}$ to t-$K_2Mo_4O_{13}$ was determined as 8.31(7) kJ/mol.

3.3. Crystal structures of the $K_2Mo_4O_{13}$ phases

Single crystals of the two $K_2Mo_4O_{13}$ phases were obtained by cooling the sample solution slowly after the hydrothermal reaction. Structures of the crystals were determined by single crystal XRD analysis.

The present cell dimensions obtained for t-$K_2Mo_4O_{13}$ are $a=7.976(2)$ Å, $b=8.345(2)$ Å, $c=10.017(2)$ Å, $\alpha=107.104(3)^\circ$, $\beta=102.885(3)^\circ$, $\gamma=109.760(3)^\circ$ that are almost the same as reported in the literature [5], but in a different setting. The cell dimensions in Ref. [5] are: $a=7.972$ Å, $b=8.352$ Å, $c=10.994$ Å, $\alpha=119.4^\circ$, $\beta=62.7^\circ$, and $\gamma=109.8^\circ$ which can be transformed as: $a'=a; b'=b; c'=-b-c$ yielding: $a=7.972$ Å, $b=8.352$ Å, $c=10.024$ Å, $\alpha=107.146^\circ$, $\beta=102.756^\circ$, and $\gamma=109.800^\circ$. The standard setting is used here. The R values were much improved in the present single crystal study, 4.4% vs. 12% for the earlier study [5]. The chain structure built up of edge-shared distorted MoO_6 octahedra, obtained for the present t-$K_2Mo_4O_{13}$ crystal, is the same as reported in the earlier study. The crystallographic data for the single crystal study is shown in Table 1.

A colorless rectangular plate, dimensions $0.17\times0.14\times0.03$ mm^3, was used for the crystal structure determination of o-$K_2Mo_4O_{13}$. The crystallographic data obtained for the phase are given in Table 2, and the crystal structure is shown in Fig. 4.

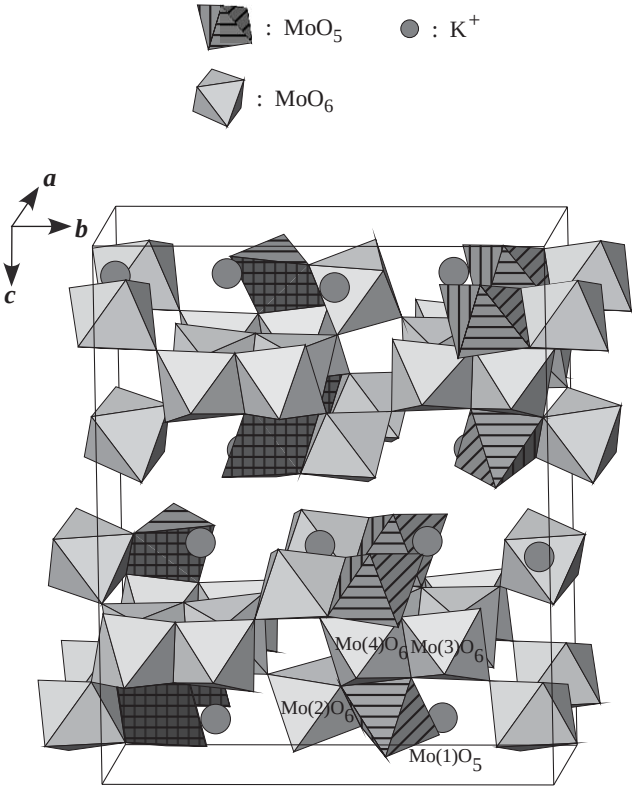

Fig. 4. Crystal structure of o-$K_2Mo_4O_{13}$.

According to the structure the phase is a layered compound characterized with a rugged sheet. The sheet consists of infinite double MoO_6 chains, built up by corner-sharing linkages of edge-shared MoO_6 (Mo(3)/Mo(4)) dimers, and edge-sharing $Mo(1)O_5/Mo(2)O_6$ dimers. The latter mixed polyhedral dimers bridge the infinite chains from alternating sides of the chains to form the rugged sheet structure. This interesting sheet structure is isostructural with $Tl_2Mo_4O_{13}$ [9] and $BaMo_4O_{13} \cdot 2H_2O$ [10].

Both (o- and t-) $K_2Mo_4O_{13}$ phases have similar infinite ribbon structures built up by corner sharing of *Z*-shaped units consisting of four edge-shared molybdenum polyhedra, as shown in Fig. 5. For t-$K_2Mo_4O_{13}$ these four polyhedra are all MoO_6 octahedra, while in o-$K_2Mo_4O_{13}$ one of the four is a MoO_5 polyhedron. In t-$K_2Mo_4O_{13}$, the polyhedra in the ribbon are almost coplanar and ribbons are linked in pairs by edge sharing to form the chain structure. In contrast, in o-$K_2Mo_4O_{13}$, the ribbons twist and are linked one after another by corner sharing of the double MoO_6 sites to form the sheet structure. The polymorphic transition observed in the present study may be related to switching over the linkages of the ribbons from corner sharing to edge sharing. For $Tl_2Mo_4O_{13}$ and $BaMo_4O_{13} \cdot 2H_2O$ no such transition has been observed. The transition from o-$K_2Mo_4O_{13}$ to t-$K_2Mo_4O_{13}$ occurs with an increase in the molar volume from 269.5 to 280.0 Å^3; the corresponding measured densities were 4.10(5) and 3.98(5) g/cm^3. The m-$K_2Mo_4O_{13}$ phase, which was not found in this synthesis study, has an intermediate density of 4.03(5) g/cm^3 [7]; its structure has not been reported.

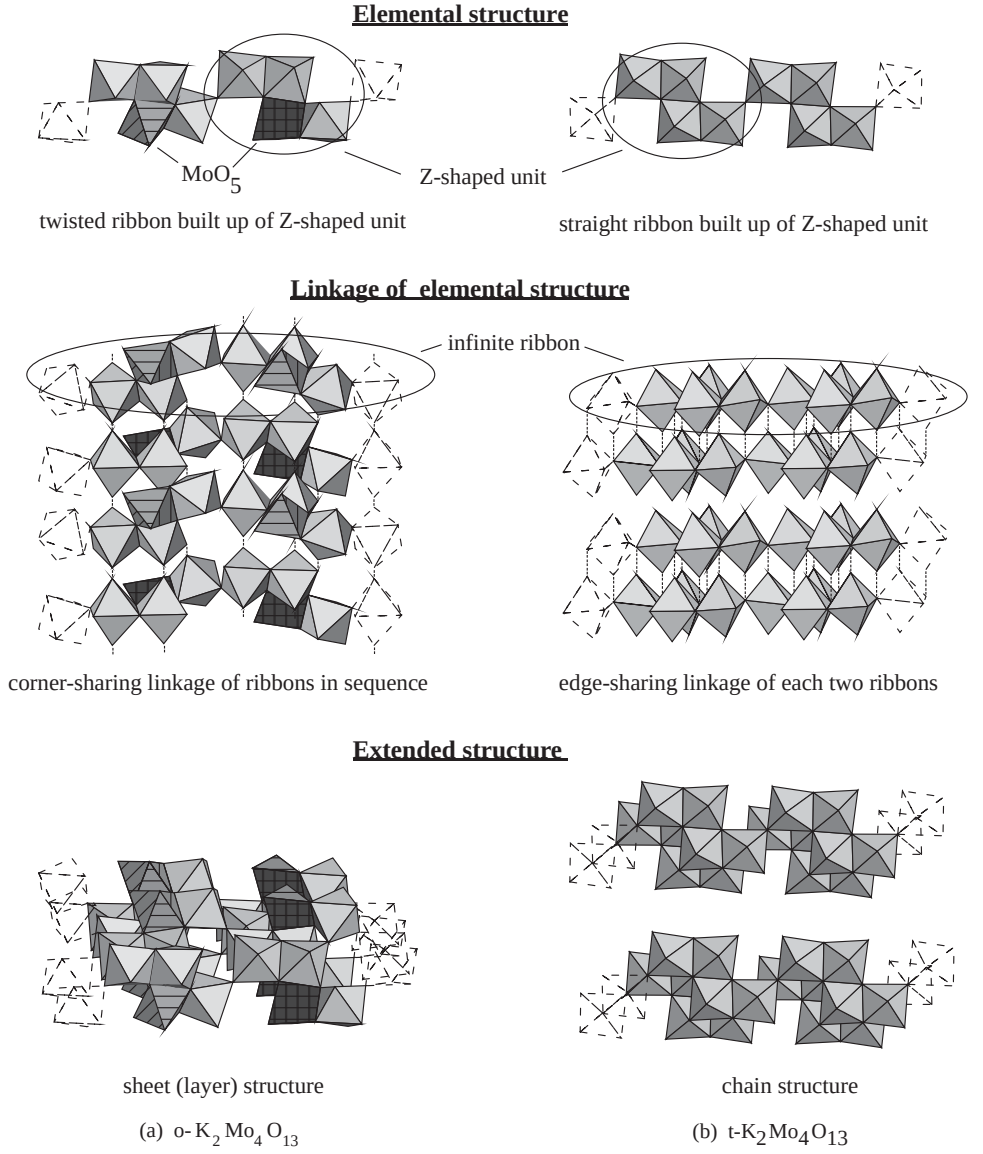

Fig. 5. Structural comparison of the two $K_2Mo_4O_{13}$ phases.

Acknowledgments

The work at Binghamton was supported by the National Science Foundation under Grant DMR0313963, and we thank Dr. Peter Zavalij for helpful discussions on the X-ray analysis and Prof. Masao Hashimoto for helpful discussions on the results of the present study.

References

[1] K. Chin, K. Eda, N. Sotani, M.S. Whittingham, J. Solid State Chem. 164 (2002) 81–87.
[2] K. Chin, Doctoral Thesis, Kobe University, 2003.
[3] L. Kihlborg, The international centre for diffraction data (ICDD) powder diffraction file (PDF), card 35-0609, Ark. Kemi 21 (1963) 357.
[4] B. Krebs, I. Paulat-Böschen, ICDD PDF, card 29-1022, Acta Crystallogr. B 32 (1976) 1697.
[5] B.M. Gatehouse, P. Leverett, ICDD PDF, Card 27-0416, J. Chem. Soc. A (1971) 2107.
[6] S. Komaba, N. Kumagai, R. Kumagai, N. Kumagai, H. Yashiro, Solid State Ionics 152–153 (2002) 319–326.
[7] J.-M. Réau, C. Fouassier, ICDD PDF, Card 24-0881, Bull. Soc. Chim. Fr. (1971) 398.
[8] P. Caillet, ICDD PDF, Card 28-0777, Bull. Soc. Chim. Fr. (1971) 4750.
[9] P. Tolédano, M. Touboul, Acta Cryst. B 34 (1978) 3547–3551.
[10] W.T. Harrison, L.L. Dussack, A.J. Jacobson, J. Solid State Chem. 116 (1995) 95–102.